Ultrasound in Med. & Biol., Vol. 48, No. 7, pp. 1290−1298, 2022

0301-5629/$ - see front matter

https://doi.org/10.1016/j.ultrasmedbio.2022.02.025

● *Original Contribution*

TOWARD FLUORO-FREE INTERVENTIONS: USING RADIAL INTRACARDIAC ULTRASOUND FOR VASCULAR NAVIGATION

HAREEM NISAR,[*,†] LEAH GROVES,[*,†] LEANDRO CARDARELLI-LEITE,[‡] TERRY M. PETERS,[*,†,§] and ELVIS C.S. CHEN[*,†,§,‖]

[*] Robarts Research Institute, Western University, London, Ontario, Canada; [†] Department of Biomedical Engineering, Western University, London, Ontario, Canada; [‡] London Health Sciences Centre, London, Ontario, Canada; [§] Department of Medical Biophysics, Western University, London, Ontario, Canada; and [‖] Lawson Health Research Institute, London, Ontario, Canada

(*Received* 19 *August* 2021; *revised* 23 *December* 2021; *in final form* 28 *February* 2022)

Abstract—Transcatheter cardiovascular interventions have the advantage of patient safety, reduced surgery time and minimal trauma to the patient's body. Transcathether interventions, which are performed percutaneously, are limited by the lack of direct line of sight with the procedural tools and the patient anatomy. Therefore, such interventional procedures rely heavily on image guidance for navigating toward and delivering therapy at the target site. Vascular navigation via the inferior vena cava, from the groin to the heart, is an imperative part of most transcatheter cardiovascular interventions including heart valve repair surgeries and ablation therapy. Traditionally, the inferior vena cava is navigated using fluoroscopic techniques such as venography and computed tomography venography. These X-ray−based techniques can have detrimental effects on the patient as well as the surgical team, causing increased radiation exposure, leading to risk of cancer, fetal defects and eye cataracts. The use of a heavy lead apron has also been reported to cause back pain and spine issues, thus leading to interventionalist's disc disease. We propose the use of a catheter-based ultrasound augmented with electromagnetic tracking technology to generate a vascular roadmap in real time and perform navigation without harmful radiation. In this pilot study, we used spatially tracked intracardiac echocardiography to reconstruct a vessel from a phantom in a 3-D virtual environment. We illustrate how the proposed ultrasound-based navigation will appear in a virtual environment, by navigating a tracked guidewire within the vessels in the phantom without any radiation-based imaging. The geometric accuracy is assessed using a computed tomography scan of the phantom, with a Dice coefficient of 0.79. The average distance between the surfaces of the two models comes out to be 1.7 ± 1.12 mm. (E-mail: hnisar3@uwo.ca)

Key Words: **Transcatheter interventions, Vascular navigation, Fluoro-free, Transfemoral guidance, Vascular disease.**

INTRODUCTION

Advances in medical imaging, combined with miniaturized and flexible procedural tools, have allowed surgical procedures to be performed percutaneously using transcatheter-based approaches. These minimally invasive approaches have increased patient safety, decreased procedure time and lowered complication rates (Jahangiri et al. 2019). Catheter-directed therapies inherently prohibit the direct line of sight with the anatomy and the tools. Interventionalists rely heavily on image guidance to navigate and position their tools to deliver therapy at the target region. Common imaging modalities used for transcatheter-based interventions include X-ray fluoroscopy, computed tomography (CT), magnetic resonance imaging (MRI), and intravascular (IVUS), intracardiac echo (ICE) or transesophageal (TEE) ultrasound (US).

Fluoroscopy is commonly used for minimally invasive procedures as it provides real-time, high-contrast vascular images by means of X-ray imaging with contrast enhancement. The radiation exposure produced by X-rays can be harmful to the patient, clinical staff and medical trainees, even when used in conjunction with various shielding techniques (Theocharopoulos et al. 2006; Christopoulos et al. 2016). The use of heavy

Address correspondence to: Hareem Nisar, Robarts Research Institute, 1151 Richmond Street North, London, Ontario N6A 5B7, Canada. E-mail: hnisar3@uwo.ca

shielding aprons may have detrimental effects on the physical health of the interventional team, causing “interventionalist’s disc disease” (Ross et al. 1997), which includes back and neck pain (Dixon et al. 2017), cervical disc herniation and other spinal and musculoskeletal issues (Goldstein et al. 2004), as well as the possibility of lead poisoning (Katsari et al. 2020). Interventional cardiologists and radiologists have reported development of eye cataracts (Jacob et al. 2013), increased risk of cancer (Roguin et al. 2013) and increased risk of fetal congenital defects (Limacher et al. 1998). The use of contrast agents to compensate for the lack of soft tissue visualization in X-rays can induce complications for patients with renal impairments and allergic reactions (Davenport et al. 2015).

Because of its high resolution and large field of view, pre-operative CT is a standard of care for vascular mapping and assessment of intravascular pathology (Murphy et al. 2018). However, CT imaging is typically used for diagnostic and pre-surgical planning and is limited in its use for real-time procedural navigation. CT is also based on ionizing radiation and carries the same risks previously described for fluoroscopy. Furthermore, the surgery cannot be performed with the patient within the CT bore. In transcatheter procedures, there is an unmet need for safe, reliable, radiation-free and real-time image guidance during vascular navigation.

In efforts to minimize the radiation exposure in catheterization laboratories, near-zero fluoro methods and no-fluoro procedural workflows have also been proposed in the literature (Stec et al. 2014; Zhang et al. 2020) to guide the catheters during an ablation procedure and perform trans-septal puncture using ICE. Alternative imaging modalities such as MR and US are also considered. Vascular navigation is fundamental to transcatheter cardiac interventions such as transcatheter aortic valve implantation (TAVI), caval valve implantation, mitral and tricuspid valve annuloplasty and repair and replacement surgeries (Prendergast et al. 2019). Accurate representation of the vessel geometry is not only important for navigation toward the target site but also for delivering the optimal therapy (Murphy et al. 2017; Shammas et al. 2019). Procedures such as angioplasty, stent placement and IVC filter placement all rely on vascular imaging to locate the pathological vessel region, select an appropriately sized device and deploy the balloon or stent correctly.

Catheter-based US technologies such as IVUS and ICE are already indispensable components of cardiac catheterization labs, assisting in the assessment of the disease and device placement. The recent introduction of optical US (opUS) technology also indicates the great potential for the use of catheter-based US for cardiovascular interventions (Little et al. 2020). US offers a radiation-free alternative for real-time image guidance. When combined with EM tracking technology, it offers the potential for a large-scale 3-D US volume reconstruction, visualization of anatomy, as well as real-time tool tracking. For most transcatheter interventions, there are two interventional phases: navigation of tools toward the target site and positioning of tools to deliver the treatment. In the case of cardiac interventions, vascular navigation is an imperative prerequisite. Either transfemoral, transradial or transjugular access is required to guide the catheters toward the heart. Inferior vena cava (IVC) navigation, from the groin to the chest, is one of the most common techniques in cardiology and is traditionally guided by fluoroscopy. In this article, the targeted clinical application is the IVC navigation performed during transcatheter cardiovascular interventions.

We propose the use of tracked US as an alternative to CT-based vascular mapping and fluoro-guided tool navigation. Instead of using radiation-based imaging to navigate the tools, we propose the following procedural workflow: Prior to the intervention, a tracked, catheter-based US probe (such as ICE, IVUS or opUS) scans the desired vasculature, and a virtual 3-D roadmap is reconstructed. This vascular path can then be easily traversed by a tracked tool or guidewire. This workflow eliminates radiation exposure and the use of heavy lead equipment. Such a system can also be used to make measurements of the vessel anatomy and intraluminal buildup. Ultrasound catheters including ICE and IVUS, as well as EM tracking technology, are already an indispensable part of a Cath Lab and are used in electrophysiology procedures. The proposed ultrasound-based workflow has several advantages over the conventional fluoroscopic techniques. Apart from the lack of radiation and heavy lead shielding equipment, an US-based navigation system offers full 3-D visualization of anatomy and provides more information to the clinician. Furthermore, the use of EM tracking technology allows for tracked tools and catheters, which can result in an engaged and informative experience for the clinicians. These features greatly reduce the cognitive load faced by the interventionalists and will potentially result in enhanced procedural outcome as well.

In this study, we used a Foresight ICE system, an intracardiac ultrasound probe that involves a single-element transducer spinning on its axis and tilted at a user-specified angle. As a result, the ultrasound image produced is a 2-D conical surface image lying in 3-D space. One of the biggest advantages of using this probe for navigation is the forward-viewing feature, which allows the clinicians to watch where they are going as they traverse the vessels, thus improving their experience and adding a layer of procedural safety. Use of the ICE probe is not limited to navigation. For transcatheter cardiac interventions, the ultrasound can further facilitate the delivery of therapy or treatment. This study is geared toward the navigation of inferior vena cava (IVC); it also has the potential to be applied to the navigation of other vessels as well. IVC has many tributaries, but they need not to be navigated for cardiac procedures. The geometry of IVC is also comparatively simpler than that of its tributaries such as hepatic veins. As the IVC passes through the entire length of the abdomen, its surrounding tissues and organs vary along the length. Thus, the appearance of the IVC in the ultrasound varies as well. All these physical and echogenic attributes of IVC are difficult to capture in one phantom. Therefore, for this first phantom study, we are illustrating the concept on an ultrasound-realistic phantom representing the infrarenal portion of the IVC. The goal is to reconstruct a vascular roadmap without any radiation, safely navigate the guidewire through the vessel and visualize the guiding catheters as they ascend toward the heart.

This article describes a pilot phantom study as a proof of concept to illustrate the idea and feasibility of a US-based vascular navigation system for transcatheter interventions. A vascular phantom was scanned and reconstructed using a forward-looking radial ICE probe and EM tracking technology. The method details, open-source implementation and phantom images are available online for reproducibility (https://github.com/hareem-nisar/VascularNavigation). The US-generated vessel model is validated against a CT scan of the vessel phantom. For a visual validation and concept demonstration of real-time guidance, we also describe navigation of a tracked guidewire in a vascular phantom using the proposed US-based approach.

METHODS

Data acquisition

A polyvinyl alcohol cryogel (PVA-C) vascular phantom was manufactured to imitate the infrarenal portion of the IVC (Nisar et al. 2020). The phantom generated realistic US imaging when scanned with intravascular (IVUS) or intracardiac (ICE) US, thus displaying a vessel-mimicking layer, blood-mimicking fluid in the lumen and a surrounding tissue-mimicking layer. In this study, a 10-Fr, forward-looking, Foresight (Conavi Medical Inc., North York, ON, Canada) ICE catheter was used to image the phantom. This probe generates 3-D conical surface images, where the angle of the cone is user adjustable. The conical images are projected on a conventional monitor screen as viewed from the apex of the cone and displayed as a circular image. A digital frame-grabber (DVI2USB 3.0, Epiphan Video, Ottawa, ON, Canada) was used to capture the projected ICE images and the cone-angle information from the console. For US tracking, the ICE probe was rigidly instrumented with a 6DoF pose sensor (Aurora, NDI, Waterloo, ON, Canada) and spatially calibrated using a point-to-line Procrustean approach (Chen et al. 2016; Nisar et al. 2019).

The vessel phantom was placed in a large water bath at room temperature (Fig. 1). The main vessel of the phantom was scanned using the tracked ICE probe at an imaging depth of 80 mm, imaging angle of 67˚ and

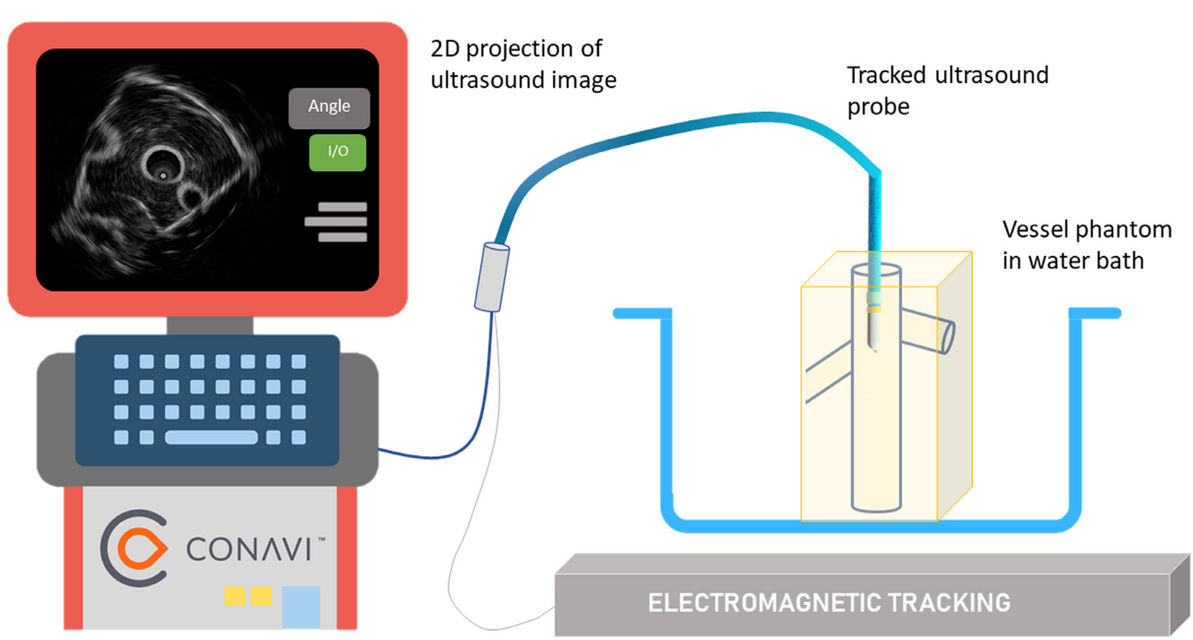

Fig. 1. Data acquisition setup. The ultrasound probe scans the vessel phantom present within the tracking space.

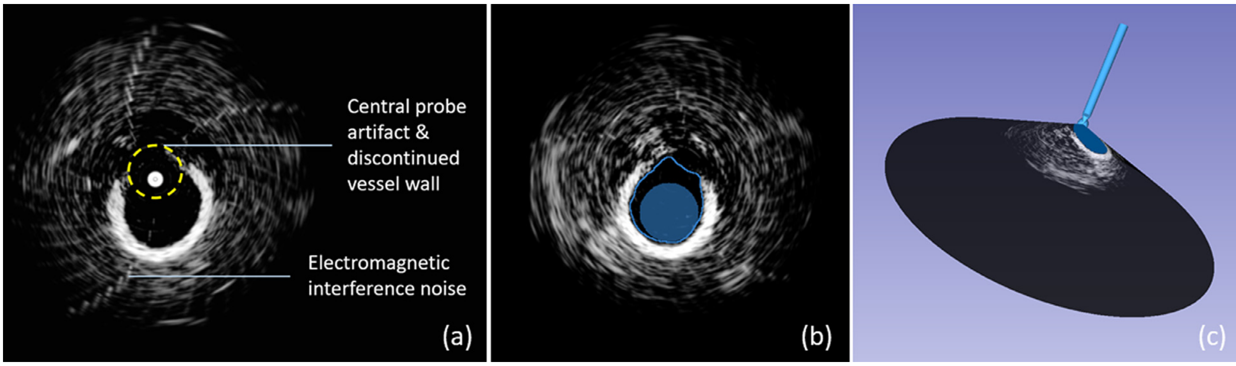

Fig. 2. (a) Image data acquired using a framegrabber as a 2-D projection of the conical ultrasound. (b) Lumen segmentation (boundary) achieved using the initial seed (solid). (c) Conical reconstruction of the ultrasound image and the lumen segmentation.

12-MHz frequency. Because of some hardware constraints in our setup, we were only able to scan the central vessel of the phantom and not the branches (details in the Discussion). US images were acquired in real time using screen capture. The imaging and tracking data were then processed to reconstruct the surface representation of the vessel from the phantom. The data acquisition, vascular roadmap generation and user interface for navigation were all implemented as an open-source software using 3D Slicer (Fedorov et al. 2012). The steps involved in the automatic generation of the 3-D vascular roadmap include pre-processing to remove image artifacts, lumen segmentation from 2-D images and reconstruction of the vessel based on the segmentations and tracking information.

Pre-processing

The acquired screen captures were cropped to remove any information outside of the US image. The bright reflections in the middle of the cropped US image represent an artifact inherent to the ICE probe (Fig. 2a). This artifact was minimized by using optimal display settings (third-level "wand" function) on the console and later masking the central bright pixels in the image in our software. The time-gain compensation settings on the console were used to suppress the reflections from the phantom boundary and the container walls. A noise-removing filter called the curve flow filter was applied to images to eliminate the interference from the EM tracker (Fig. 2a) while preserving the contours of the vessel boundary. This was a necessary step prior to performing image processing for lumen segmentation.

Lumen segmentation

Distinct from imaging using a hand-held percutaneous US transducer, the shape of the vessel wall can vary significantly for catheter-based US. As the US catheters travel through the vasculature adhering close to the vessel wall, the wall does not always appear as a closed circle in the case of radial IVUS and ICE imaging. The first few millimeters of ICE imaging are corrupted by a ring artifact inherent to the radial ICE probe (Fig. 2a). As such, when the ICE catheter is clinging to the vessel wall, the reflection is interrupted close to the center of the image (Fig. 2a), and the vessel boundary appears C-shaped. Therefore, in this study, an edge-based approach was used to segment the vessel lumen from the ICE images, minimizing the error/leakages caused by a discontinuous vessel boundary. A statistics-based active contour algorithm was applied (Gao et al. 2010). This algorithm grows the boundaries of an initial seed based on the characteristics of the underlying image intensities, and can be manipulated by the parameters - intensity homogeneity (set to 0.8) and boundary smoothness (set to 1) to maintain the roundness of the contour and minimize leakage based on intensity.

The performance of the segmentation algorithm is highly dependent on the size and placement of the initial seed. Therefore, for the algorithm to be effective, it is necessary to have an initial seed, closely fitted to and completely encapsulated and centered within the vessel lumen (Gao et al. 2010). The Hough transform was used to approximate the initial seed by fitting a circle to the lumen (Fig. 2b) (parameter values: Hough gradient, dp = 1, min_dist = 100, param1 = 95, param2 = 20). Gaussian blur was applied prior to the Hough transform to avoid overdetection of circles. To ensure that the seed does not overlap with the vessel boundary, the fitted circle was iteratively decreased in radius until there were no bright reflections in the underlying image. One hundred and eighty image frames were processed, and 2-D lumen segmentations were acquired for each image.

Vessel reconstruction

The Foresight ICE probe generates forward-looking conical surface images. The images acquired by this device, and subsequently the lumen segmentation, were

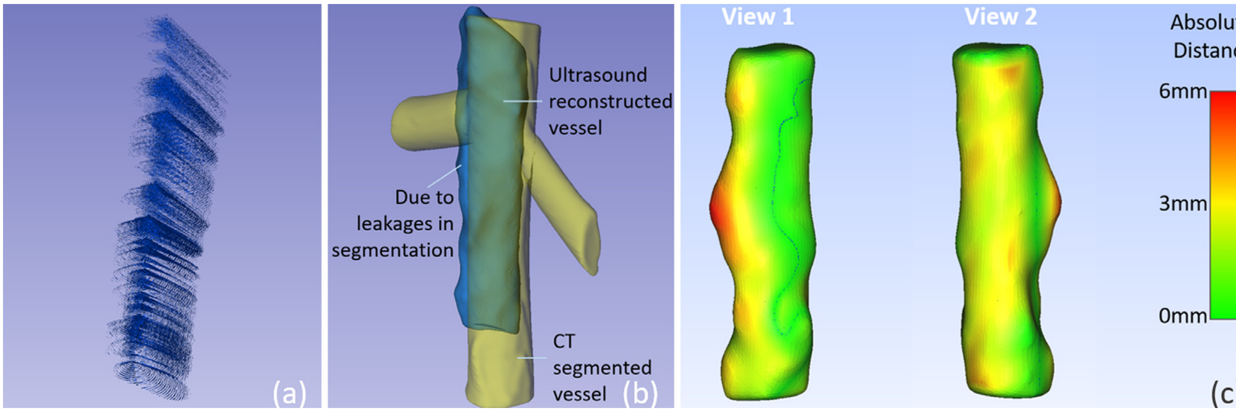

Fig. 3. (a) Skeleton of the vessel composed of spatially calibrated segmentations. (b) Ultrasound reconstruction registered to the segmented computed tomography (CT) scan of the phantom. (c) Visualization of the surface-to-surface distance analysis between the ultrasound and CT models.

a version of the true US data projected onto a 2-D disk. Two-dimensional lumen segmentations were subjected to 3-D conversion to reconstruct true, conical segmentations (Fig. 2c) using the radius and imaging angle information, available through the console. This reconstruction is governed by the equation

$$\begin{bmatrix} x_{3D} \\ y_{3D} \\ z_{3D} \end{bmatrix} = \begin{bmatrix} 1 & 0 & -o_x \\ 0 & 1 & o_y \\ 1 & 0 & \| (x_{2D}), y_{2D}) \| \cdot \tan(90-\varphi) \end{bmatrix} \begin{bmatrix} x_{2D} \\ y_{2D} \\ 1 \end{bmatrix} \quad (1)$$

where (o_x, o_y) represents the center of the planar image or the apex of the conical image, and φ represents the imaging angle of the cone-shaped image. Each segmentation was positioned and scaled to its correct shape and location in 3-D space by applying US probe calibration and tracking information, producing a skeleton of the vessel (Fig. 3a). The vessel skeleton was then processed to form a closed 3-D surface representation using binary morphological closing, with an annulus kernel of size [60,60] to fill the gaps between consecutive segments. For final smoothing of the reconstructed vessel, a Gaussian blur with a standard deviation of 3 was applied. The result represents the 3-D model of the vessel scanned from our phantom (Fig. 3b), spatially present in the EM trackers' coordinate system.

Validation

As described previously, vascular navigation is currently achieved using fluoroscopy or CT mapping. The vessel phantom was imaged using US, and the vessel was reconstructed and compared with X-ray and CT. Geometric accuracy of the US-reconstructed vessel model was validated against the vessel segmented from the CT scan of the same phantom. The absolute surface-to-surface distance between the two models was computed after a rigid registration (Besl and McKay 1992). For vascular navigation, one of the clinically relevant goals is to know the overall alignment of the vessels in space. To evaluate the spatial alignment, we used Dice metrics, which compares the spatial overlap between the reconstructed and CT vessel after CT-US registration is performed. A false-positive spatial region in the reconstructed US vessel is also an important metric and must be minimal to avoid the misrepresentation of the vessel. For many vascular procedures, the clinical objective is to avoid puncturing the vessels. In such cases, boundary accuracy becomes important, as do the false-positive regions. To evaluate the contours of the reconstructed vessel, we calculated the Hausdorff distance (HD) metrics (Taha and Hanbury 2015). Volumetric analysis was not performed as volume-based metrics are invariant of segmentation shape and boundary and thus can be misleading. As a visual validation, we determined what US-based navigation may look like. A tracked, straight-tip guidewire (Piazza et al. 2020), augmented with a 5-DOF EM sensor, was maneuvered to navigate the vessels in the phantom.

RESULTS

The absolute distance between the US-reconstructed vessel and the registered CT-segmented vessel was computed and presented as a heatmap on the vessel surface in Figure 3c. The average distance between the surfaces of the two models comes out to be 1.7 ± 1.12 mm. A maximum error of 5.86 mm between the two surface models was observed. The spatial overlap between the registered US and CT models was evaluated using the Dice coefficient, sensitivity and specificity measures where

$$\text{Dice} = \frac{\text{true positive overlap between CT and US vessels}}{(\text{number of voxels/CT vessel}) \times (\text{number of voxels/US vessel})} \quad (2)$$

The spatial distance between the two model boundaries was evaluated using the HD. The geometric accuracy results are reported in Table 1. Comparison revealed that the US model had 12.93% false-negative and 6.60% false-positive spatial overlap.

X-ray imaging of our phantom, along with a guidewire, is represented in Figure 4a. In comparison, we can also achieve tool guidance using an US-guided vascular navigation system. Figure 4b illustrates what the US-reconstructed vessel looks like in 3-D space. Virtual representation of a tracked guidewire can be seen in context, as it navigates the phantom vessel.

DISCUSSION

In this article, we have described a vascular reconstruction−based navigation system, which provides a safe and radiation-free method for guiding tools during transcatheter procedures. An EM-tracked ICE US probe was used to reconstruct the vascular path in a phantom, such that it can be visualized in a common coordinate system with a tracked guidewire for vessel navigation.

Table 1. Metrics used to quantify the spatial overlap and boundary accuracy of the ultrasound-reconstructed vessel compared with the vessel segmented from the computed tomography scan of the phantom

Spatial overlap	Value	Hausdorff distance (mm)	Value
Dice coefficient	0.79	Maximum	5.86
Sensitivity	0.70	Average	1.63
Specificity	0.88	95%	3.16

The results indicate that the average error in terms of HD is 1.7 mm, with a 3.16 mm confidence interval, which is a clinically acceptable value (Linte et al. 2012). During navigation, it is important to identify the vessel boundary and the regions outside the vessel lumen so as to not puncture or damage the vessel wall. Our results indicate that only 6.60% of the region lies outside the ground truth provided by the CT scan of the phantom. This oversegmentation is due to the leakage through the discontinuous wall boundary in some of the images when the ultrasound probe is clinging to the vessel wall. The accuracy of the navigation system can further be improved by improving the segmentation and tracking accuracy as discussed below.

The resulting error is a combination of many different errors in the system, such as EM tracking inaccuracies, propagation of calibration errors, US probe hardware constraints, registration errors and relative motion of the phantom if any. One of the major limitations of our study is defined by sensorizing the US probe and its calibration accuracy. This inaccuracy can be minimized by applying a manual offset correction for the imaging angle. The ICE probe used in this study has a small diameter of 3.3 mm, which required rigidly fixing the sensor on the outer sheath of the probe, farther away from the origin of the image. The rigid and outer positioning of the sensor led to some hardware constraints, resulting in our inability to turn and guide the probe into the branches of the vessel. This limitation is strictly a characteristic of our experimental setup in this preliminary study using a Foresight ICE probe. The proposed idea can be extended to other radial ultrasound catheters as well. Ideally the tracking sensor should be integrated within the US catheter and pre-calibrated by the manufacturers to eliminate any limitation to maneuvering the US. For a clinical system, the EM sensor must be integrated inside the US catheter to achieve accuracy in tracking, freedom in motion and patient safety from an active element. In the future, we

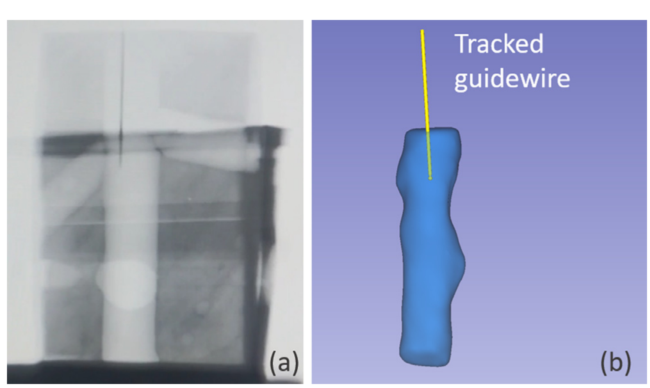

Fig. 4. An example use case for navigating a tracked guidewire within the ultrasound-reconstructed vessel (b) as compared with the fluoroscopic equivalent (a).

plan to collaborate with the ICE probe manufacturers to acquire ICE probes embedded with EM sensors and design a prototype of the US guidance system presented as a concept study in this article.

The proposed US-based vascular navigation system can be implemented using many catheter-based US technologies, such as radial IVUS probes that are regularly used during cardiac and endovascular interventions. Other than tracking, the accuracy of a clinical vessel reconstruction algorithm also largely depends on the accuracy of lumen segmentation from *in vivo* imaging. The appearance of a vessel in an intravascular or intracardiac US image varies significantly depending on the size and composition of the vessel, as well as the surrounding tissue and organs. The phantom images presented in this study replicate the US imaging of the infrarenal portion of the IVC only. Even the echogenicity of the IVC changes as it passes through the abdomen. Thus, a clinical system, implementing the proposed idea of US navigation, will require a robust deep learning–based segmentation pipeline, which is capable of accurately identifying and segmenting all vascular structures as well as vessel branches and tributaries. Existing network architectures, such as U-Net, might be a suitable option for medical image segmentation. As this is a pilot, proof-of-concept study for navigation with relatively restricted imaging data, we did not include any learning-based approaches for segmentation and relied on conventional image processing techniques.

In future work we aim to improve this vascular reconstruction pipeline by replacing the image processing–based vessel segmentation algorithm with a deep learning–based segmentation technique trained on animal images acquired using the forward-looking Foresight ICE probe. The use of machine learning for vascular segmentation and reconstruction has been previously performed using both surface US scans (Yang et al. 2013; Groves et al. 2020) and intravascular US (Yang et al. 2018). The integration of a machine learning–based segmentation will allow for accurate patient-specific reconstructions to be obtained that account for differences in patient pathology. The segmentation algorithm can be trivially replaced within our vascular reconstruction pipeline such that the different vessels required for navigation can be reconstructed using a robust segmentation algorithm capable of delineating various vascular morphologies and side vessel branches, allowing for safe navigation from the insertion site to the central venous system.

The phantom-based workflow described in this article is time consuming because of the computationally expensive vessel segmentation technique used. For clinical purposes, the vessel segmentation step should be fast and robust. However, this is a first proof-of-concept study, and the vessel segmentation step is suitable only for the phantom images. Therefore, to replace the current vessel segmentation step, we have developed a real-time segmentation technique for isolating vessel lumina from ultrasound imaging of inferior vena cava in animals Nisar et al., 2022. We are also currently working toward optimizing the presented pipeline to perform the vessel reconstruction on the order of seconds. Combining the optimized reconstruction algorithm with the real-time vessel segmentation method will enable a time-apt image guidance system ready for pre-clinical studies.

The accuracy of the vessel reconstruction algorithm described in this article depends largely on the accuracy of the vessel segmentation and the tracking technology used. The electromagnetic tracking has submillimeter accuracy; however, the vessel segmentation does not. As mentioned earlier, we have developed a real-time vessel segmentation method using deep learning. This new segmentation method relies on a trained U-Net model to accurately segment the complex-shaped vessel lumina from the ICE imaging of the vena cava from a swine. This deep learning–based method is robust against boundary artifacts such as intraluminal buildups and stents. However, the algorithm produces inaccurate segmentation when a lead is present inside the vessel. Any artifacts outside the vessel and present in the surrounding tissue do not have a significant impact on the accuracy of our vessel segmentation and reconstruction. To cater to any artifacts, the new segmentation technique can be trivially modified without disturbing the entire reconstruction pipeline described in this article. Deep learning–based systems benefit from a variety of imaging data sets in making the segmentation algorithm more robust. By retraining the U-Net model on different examples of vascular imaging with artifacts, the segmentation and thus the reconstruction can be made robust and accurate.

Another limitation is the size of the US catheter. The US probe used in this study is a 10-Fr device, which is large and less suitable for the arterial system, although it is usually not problematic for venous interventions. This is a limitation of the current technology (Foresight ICE probe by Conavi Medical Inc.), and ideally this device will be miniaturized by the manufacturers in the near future. The workflow described in this article can potentially be adapted for IVUS imaging, in which the catheter is much smaller. For example, the Novasight Hybrid (by Conavi Medical Inc.) is a combined IVUS-OCT imaging catheter with a size of 3.3 French (Ono et al. 2020).

CONCLUSIONS

Transcatheter interventions provide a low-impact means of delivering therapy using miniaturized equipment and medical imaging technologies. Vascular navigation is a ubiquitous process as it is a prerequisite to reach the target organ or target site in another vessel. The current standard of care employs fluoroscopic techniques or the use of CT vascular mapping, both of which come at the cost of radiation exposure and wearing heavy, shielding aprons. Through this study, we aim to initiate a discussion on the merits of moving toward the use of US-based instead of radiation-based techniques for transcatheter and endovascular interventions. We present a proof-of-concept study to use catheter-based US technology, equipped with tracking sensors, to create a vascular roadmap. Results indicate that the geometric accuracy is comparable to that observed in CT mapping. The concept demonstration (Fig. 4) reveals side by side that a US-guided system can provide the same level of information and in three dimensions without the hazards of radiation and lead shielding.

Acknowledgments—The authors thank Dan Bainbridge (London Health Sciences Centre) and John Moore (Archetype Biomedical Inc.) for their valuable discussion and insight into the project. We acknowledge our sources of funding: the Canadian Institutes of Health Research (CIHR) and Canadian Foundation for Innovation (CFI). The grants are held by Terry Peters. The authors also thank Conavi Medical Inc. for providing the ultrasound imaging data set.

REFERENCES

Besl P, McKay ND. A method for registration of 3-D shapes. IEEE Trans Pattern Anal Mach Intell 1992;14:239–256.

Chen ECS, Peters TM, Ma B. Guided ultrasound calibration: where, how, and how many calibration fiducials. Int J Comput Assist Radiol Surg 2016;11:889–898.

Christopoulos G, Makke L, Christakopoulos G, Kotsia A, Rangan BV, Roesle M, Haagen D, Kumbhani DJ, Chambers CE, Kapadia S, Mahmud E, Banerjee S, Brilakis ES. Optimizing radiation safety in the cardiac catheterization laboratory. Catheterization Cardiovasc Interventions 2016;87:291–301.

Davenport MS, Cohan RH, Ellis JH. Contrast media controversies in 2015: Imaging patients with renal impairment or risk of contrast reaction. AJR Am J Roentgenol 2015;204:1174–1181.

Dixon RG, Khiatani V, Statler JD, Walser EM, Midia M, Miller DL, Bartal G, Collins JD, Gross KA, Stecker MS, Nikolic B. Society of Interventional Radiology: Occupational back and neck pain and the interventional radiologist. J Vasc Interventional Radiol 2017;28:195–199.

Fedorov A, Beichel R, Kalpathy-Cramer J, Finet J, Fillion-Robin JC, Pujol S, Bauer C, Jennings D, Fennessy F, Sonka M, Buatti J, Aylward S, Miller JV, Pieper S, Kikinis R. 3D Slicer as an image computing platform for the Quantitative Imaging Network. Magn Reson Imaging 2012;30:1323–1341.

Gao Y, Tannenbaum A, Kikinis R. Simultaneous multi-object segmentation using local robust statistics and contour interaction. In: Menze B, Langs G, Tu Z, Criminisi A, (eds). Medical Computer Vision. Recognition Techniques and Applications in Medical Imaging. : Lecture Notes Comput Sci; 2010 195203. MCV 20106533.

Goldstein JA, Balter S, Cowley M, Hodgson J, Klein LW. Occupational hazards of interventional cardiologists: Prevalence of orthopedic health problems in contemporary practice. Catheterization Cardiovasc Interventions 2004;63:407–411.

Groves LA, VanBerlo B, Veinberg N, Alboog A, Peters TM, Chen EC. Automatic segmentation of the carotid artery and internal jugular vein from 2D ultrasound images for 3D vascular reconstruction. Int J Comput Assist Radiol Surg 2020;15:1835–1846.

Jacob S, Boveda S, Bar O, Brezin A, Maccia C, Laurier D, Bernier MO. Interventional cardiologists and risk of radiation-induced cataract: Results of a French multicenter observational study. Int J Cardiol 2013;167:1843–1847.

Jahangiri M, Hussain A, Akowuah E. Minimally invasive surgical aortic valve replacement. Heart 2019;105:s10–s15.

Katsari K, Paraskevopoulou C, Barati M, Kostopoulou E, Griskevicius R, Blazquez N, Tekin HO, Illing RO. Lead exposure in clinical imaging—The elephant in the room. Eur J Radiol 2020;131 109210.

Limacher MC, Douglas PS, Germano G, Laskey WK, Lindsay BD, McKetty MH, Moore ME, Park JK, Prigent FM, Walsh MN, Forrester JS, Faxon DP, Fisher JD, Gibbons RJ, Halperin JL, Hutter AM, Kaul S, Skorton DJ, Weintraub WS, Winters WL, Wolk MJ. Radiation safety in the practice of cardiology. Technical Report, 1998.

Linte CA, Lang P, Rettmann ME, Cho DS, Holmes DR, Robb RA, Peters TM. Accuracy considerations in image-guided cardiac interventions: Experience and lessons learned. Int J Comput Assist Radiol Surg 2012;7:13.

Little CD, Colchester RJ, Noimark S, Manmathan G, Finlay MC, Desjardins AE, Rakhit RD. Optically generated ultrasound for intracoronary imaging. Front Cardiovasc Med 2020;7 525530.

Murphy EA, Ross RA, Jones RG, Gandy SJ, Aristokleous N, Salsano M, Weir-McCall JR, Matthew S, Houston JG. Imaging in vascular access. Cardiovasc Eng Technol 2017;8:255–272.

Murphy DJ, Aghayev A, Steigner ML. Vascular CT and MRI: A practical guide to imaging protocols. Insights Imaging 2018;9:215–236.

Nisar H, Carnahan PK, Fakim D, Akhuanzada H, Hocking D, Peters TM, Chen ECS. Towards ultrasound-based navigation: deep learning based IVC lumen segmentation from intracardiac echocardiography. Proc. SPIE 12034, Medical Imaging 2022: Image-Guided Procedures, Robotic Interventions, and Modeling 2022;1203422 In this issue.

Nisar H, Moore J, Alves-Kotzev N, Hwang GYS, Peters TM, Chen ECS. Ultrasound calibration for unique 2.5D conical images. In: Fei B, Linte CA, (eds). Medical Imaging 2019: Image-Guided Procedures, Robotic Interventions, and Modeling. : SPIE; 2019. p. 78.

Nisar H, Moore J, Piazza R, Maneas E, Chen ECS, Peters TM. A simple, realistic walled phantom for intravascular and intracardiac applications. Int J Comput Assist Radiol Surg 2020;15:1513–1523.

Ono M, Kawashima H, Hara H, Gao C, Wang R, Kogame N, Takahashi K, Chichareon P, Modolo R, Tomaniak M, Wykrzykowska JJ, Piek JJ, Mori I, Courtney BK, Wijns W, Sharif F, Bourantas C, Onuma Y, Serruys PW. Advances in IVUS/OCT and future clinical perspective of novel hybrid catheter system in coronary imaging. Front Cardiovasc Med 2020;7:119.

Piazza R, Nisar H, Moore J, Condino S, Ferrari M, Ferrari V, Peters T, Chen ECS. Towards electromagnetic tracking of J-tip guidewire: Precision assessment of sensors during bending tests. In: Fei B, Linte CA, (eds). Medical Imaging 2020: Image-Guided Procedures, Robotic Interventions, and Modeling. : SPIE; 2020. p. 5.

Prendergast BD, Baumgartner H, Delgado V, Gerard O, Haude M, Himmelmann A, Iung B, Leafstedt M, Lennartz J, Maisano F, Marinelli EA, Modine T, Mueller M, Redwood SR, Rörick O, Sahyoun C, Saillant E, Søndergaard L, Thoenes M, Thomitzek K, Tschernich M, Vahanian A, Wendler O, Zemke EJ, Bax JJ. Transcatheter heart valve interventions: where are we? Where are we going?. Eur Heart J 2019;40:422–440.

Roguin A, Goldstein J, Bar O, Goldstein JA. Brain and neck tumors among physicians performing interventional procedures. Am J Cardiol 2013;111:1368–1372.

Ross AM, Segal J, Borenstein D, Jenkins E, Cho S. Prevalence of spinal disc disease among interventional cardiologists. Am J Cardiol 1997;79:68–70.

Shammas N, Radaideh Q, Shammas WJ, Daher GE, Rachwan RJ, Radaideh Y. The role of precise imaging with intravascular ultrasound in coronary and peripheral interventions. Vasc Health Risk Manage 2019;15:283–290.

Stec S, Sledz J, Mazij M, Ras M, Ludwik B, Chrabaszcz M, Sledz A, Banasik M, Bzymek M, Mlynarczyk K, Deutsch K, Labus M, Spikowski J, Szydlowski L. Feasibility of implementation of a simplified, no-X-ray, no-lead apron, two-catheter approach for ablation of supraventricular arrhythmias in children and adults. J Cardiovasc Electrophysiol 2014;25:866–874.
Taha AA, Hanbury A. Metrics for evaluating 3D medical image segmentation: analysis, selection, and tool. BMC Medical Imaging 2015;15:29.
Theocharopoulos N, Damilakis J, Perisinakis K, Manios E, Vardas P, Gourtsoyiannis N. Occupational exposure in the electrophysiology laboratory: quantifying and minimizing radiation burden. Br J Radiol 2006;79:644–651.
Yang X, Jin J, Xu M, Wu H, He W, Yuchi M, Ding M. Ultrasound common carotid artery segmentation based on active shape model. Comput Math Methods Med 2013; 345968.
Yang J, Tong L, Faraji M, Basu A. IVUS-Net: An intravascular ultrasound segmentation network. International Conference on Smart Multimedia. Cham, Switzerland. : Springer; 2018. p. 367–377.
Zhang G, Cheng L, Liang Z, Zhang J, Dong R, Hang F, Wang X, Wang Z, Zhao L, Wang Z, Wu Y. Zerofluoroscopy transseptal puncture guided by right atrial electroanatomical mapping combined with intracardiac echocardiography: A single center experience. Clin Cardiol 2020;43:1009–1016.